Korean J. Chem. Eng., **19**(3), 510-518 (2002)

Catalytic Growth of Semiconductor Micro- and Nano-crystals using Transition Metal Catalysts

Kee Suk Nahm†, Young Hwan Mo, Md. Shajahan and Sang Hyun Lee

School of Chemical Engineering and Technology, Chonbuk National University, Chonju 561-756, Republic of Korea
(*Received 4 December 2001 • accepted 9 March 2002*)

Abstract—The catalytic reaction concept was introduced in the growth of semiconductor micro- and nano-crystals. It was found that gallium nitride (GaN) micro- and nano-crystal structures, carbon nanaotubes, and silicon carbide (SiC) nanostructures could be efficiently grown using transition metal catalysts. The use of Ni catalyst enhanced the growth rate and crystallinity of GaN micro-crystals. At 1,100 °C, the growth rate of GaN micro-crystals grown in the presence of Ni catalyst was over nine times higher than that in the absence of the catalyst. The crystal quality of the GaN micro-crystals was almost comparable to that of bulk GaN. Good quality GaN nanowires was also grown over Ni catalyst loaded on Si wafer. The nanowires had 6H hexagonal structure and their diameter was in the range of 30-50 nm. Multi-wall nanotubes (MWNTs) were grown over 20Fe : 20Ni : 60Al_2O_3 catalyst. However, single wall nanotubes (SWNTs) were grown over 15Co : 15Mo : 70MgO catalyst. This result showed that the structure of CNTs could be controlled by the selection of catalysts. The average diameters of MWNTs and SWNTs were 20 and 10 nm, respectively. SiC nanorod crystals were prepared by the reaction of catalytically grown CNTs with tetrametysilane. Structural and optical properties of the catalytically grown semiconductor micro- and nano-crystals were characterized using various analytic techniques.

Key words: Catalytic Growth, Micro- and Nano-Crystals, GaN, MWNT, SWNT, SiC

INTRODUCTION

Catalysts have been widely utilized in most chemical reactions currently employed in chemical plants because most catalysts enhance the yield of chemical reactions significantly by promoting the reaction rate through different molecular mechanisms. However, the use of catalysts in semiconductor manufacturing processes has been strongly prohibited because people believed catalysts play a role as impurities in semiconductor materials, leading to the deterioration of device performance.

Recently, some reports on the utilization of catalysts in semiconductor crystal growth have begun to emerge in the scientific papers. Polycrystalline silicon (poly-Si) thin film has been a key material for large-area electronic devices for flat-panel displays and solar cells. Poly-Si is generally made from amorphous silicon (a-Si) thin film by various crystallization techniques. Although a number of techniques have been proposed during the past several years to achieve the crystallization of a-Si to poly-Si on large-area glass substrate [Iverson and Reif, 1987; Im and Sposili, 1996; Yoon et al., 2001], a solid phase crystallization is a common method to crystallize amorphous silicon (a-Si) to poly-Si because of its unique advantages such as low manufacturing cost and uniformity over large area [Iverson and Reif, 1987]. However, its crystallization temperature is too high for use of large-area glass substrate. Literature has reported that some metals, such as Al, Ni or Pd, act as a catalyst in the crystallization of a-Si into poly-Si so that the crystallization can be realized at relatively low temperatures less than 400 °C [Jang et al., 1998].

The growth of carbon nanotubes (CNTs) is a typical example for the application of catalysts to semiconductor crystal growth. Owing to the extraordinary properties of carbon nanotubes such as a metal, semiconductor and superconductor [Hassanien et al., 1998], and in parallel their hydrogen storage capability [Dillon et al, 1997; Kibria et al., 2001], the synthesis and application of CNTs have been intensively investigated since their discovery in 1991 [Iijima, 1991]. Carbon nanotubes have been synthesized by numerous techniques, namely, arc-discharge [Maser et al., 1996], laser ablation [Guo et al., 1995], catalytic chemical vapor deposition, etc. [Ivanov et al., 1995; Kibria et al., 2002]. Most of the growth processes above employ some metal catalysts to grow CNTs. Fe, Ni and Co supported catalysts have been the most commonly employed catalysts, but variety of new catalysts have been examined to get desired CNT structures [Iijima and Ichihashi, 1993; Bethune et al., 1993; Saito et al., 1993].

The wide-band-gap semicondutor GaN is currently of great interest for development of optoelectronic devices at blue and near-ultraviolet wavelengths [Akasaki and Amano, 1997] as well as high temperature and high-frequency electronics [Kim et al., 1997]. Due to the continual demands for reduction in device size, it is naturally of interest to fabricate nanodevices based on nanoscale materials with novel properties. GaN micro- and nano-crystals are good candidates for these needs [Gonsalves et al., 1997; Koo et al., 2001]. GaN micro-crystals have lately synthesized using various methods [Porowski, 1996; Shibata et al., 1999]. However, most of the works still remained in the fundamental study on the growth of high quality GaN crystal. Recently, our laboratory has reported the growth of high quality GaN micro-crystals using Ni catalyst by a direct reaction of gallium and ammonia [Nahm et al., 2000; Lee et al., 2001].

†To whom correspondence should be addressed.
E-mail: nahmks@moak.chonbuk.ac.kr
‡This paper is dedicated to Professor Wha Young Lee on the occasion of his retirement from Seoul National University.

A number of techniques have been also proposed during the past several years to achieve the growth of 1-dimensional semiconductor GaN nanowires [He et al., 2001; Chen et al., 2001]. However, a synthesis of GaN nanowires by the catalytic reaction of gallium and ammonia using transition metals has been proposed by Chen et al. this year [Chen et al., 2001]. Recent successful fabrication of CNT transistors achieved by IBM group nourishes the importance of one dimensional semiconductor crystal nanostructures for the future nanodevice fabricaltion [Derycke et al., 2001]. Likewise, other research group also observed the enhanced growth rate of semiconductor crystal growth, but they did not realize that it was due to the catalytic activity of the metal species involved in the growth reactions [Gu et al., 2000; Xie et al., 1996].

Subsequently, the use of catalysts in semiconductor crystal growth can make a breakthrough to achieve high purity and quality semiconductor growth as well as to control of the crystal structure intentionally by examining the catalytic growth mechanism precisely. In spite of concrete evidence for the catalytic effect in the growth of semiconductor crystals observed above, insufficient recognition of catalyst importance in the crystal growth still prevents a widespread of catalyst application to the growth of semiconductor crystals.

In this work, we report the growth of GaN micro- and nano- crystal structures, carbon nanaotubes, and SiC nanostructures using transition metal catalysts to introduce the catalytic growth of semiconductor crystals. Structural and optical properties of the catalytically grown semiconductor crystals were characterized using various analytic techniques.

EXPERIMENTS

1. GaN Micro-Crystals and GaN Nanowires

GaN micro-crystals were grown by a direct reaction of molten Ga and ammonia gas using a Ni-mesh catalyst. The growth of the GaN crystals was carried out in a homemade quartz tubular reactor heated in a tubular furnace (Fig. 1). The growth temperature was monitored with a Rh/Pt thermocouple from the bottom of the reactor and controlled by a temperature controller. Cylindrical Ni-mesh catalyst (0.6 g) was placed between the gas delivery tube and inner reactor tube. Small pieces of solid Ga (8 g, 99.99%) were loaded in the inner quartz reactor. The reactor was evacuated to 10^{-4} torr for 30 minutes and then purged with 100 sccm N_2 (9N). This procedure was repeated more than five times to remove the residual impurities in the reactor. The reactor pressure was adjusted using N_2 to be one atmosphere. After elevating the reactor temperature to 800 °C in the flow of N_2 gas, the N_2 flow was stopped, switched to 100 sccm H_2 gas (9 N), and the temperature maintained for 5 min to clean the Ni catalyst surface. The reactor temperature was again raised from 800 °C to the growth temperature and then the hydrogen gas was completely changed to 50 sccm NH_3 (99.99%). All the gases were introduced into the reactor through the delivery tube and the Ni catalyst was completely dipped in the Ga melt during the growth. The growth reaction was performed at various temperatures (1,000-1,100 °C). After the growth reaction, the temperature was slowly cooled to room temperature in the flow of NH_3 gas. The GaN crystals were removed from the as-grown mixture by dissolving unreacted Ga and Ni catalyst in HCl solution. The separated GaN crystals were washed with distilled water and dried in a vacuum oven.

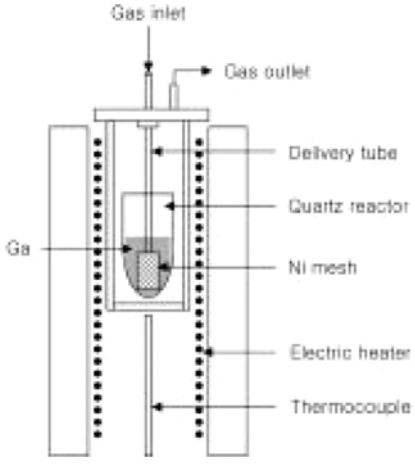

Fig. 1. A schematic diagram of the growth reactor for GaN microcrystals and GaN nanowires.

GaN nanowires were grown by a direct reaction of molten Ga and ammonia gas on Si wafer loaded Ni catalyst. Ni catalyst was loaded on Si wafer by dipping into 8.6 M $Ni(NO_3)_3 \cdot 9H_2O$ solution. A Si substrate (8 cm×0.5 cm) was vertically set up in the reactor and half of the substrate was exposed above the surface of Ga liquid to grow GaN nanowires. The GaN nanowires were grown for 5 hr at 910 °C and 1 atm with 20 sccm NH_3 in the same reactor. The growth sequence of the GaN nanowire crystals was equal to that of GaN micro-crystals.

2. Carbon Nanotubes and SiC Nanorods

For the growth of CNTs, two bimetallic catalysts of compositions 20Fe : 20Ni : 60Al_2O_3 and 15Co : 15Mo : 70MgO were prepared by an impregnation method. The α-Al_2O_3 and MgO powders used as the catalyst supports had average diameters of 0.3 and 0.5 μm, respectively. High metal loading was chosen in order to get longer catalytic activity. To prepare 20Fe : 20Ni : 60Al_2O_3 catalyst, aqueous solutions of $Fe(NO_3)_3 \cdot 9H_2O$ and $Ni(NO_3)_2 \cdot 6H_2O$ having required amount of metals were mixed with Al_2O_3 powders and stirred for 1 h at 60 °C to remove dissolved oxygen and to get homogeneous impregnation of metal salts in the support. The impregnate was then dried in an oven at 100 °C for 12 h, calcined at 400 °C for 4 h in a box furnace and reduced in 100 sccm hydrogen flow at 450 °C for 3 h under vacuum. The prepared catalysts were stored in sealed vessels and CNTs were synthesized over the catalysts. 15Co : 15Mo : 70MgO catalyst was prepared along the same sequence with the 20Fe : 20Ni : 60Al_2O_3 catalyst except using $Co(NO_3)_2 \cdot 6H_2O$ and $(NH_4)_6Mo_7O_{24} \cdot 4H_2O$ for precursors.

The growth of the CNTs was carried out in a rapid thermal chemical vapor deposition (RTCVD) reactor described in elsewhere [Seo et al., 1997]. Approximately 40 mg of a catalyst sample was uniformly dispersed in the base area of a quartz plate and placed in the central region of a horizontal quartz tube reactor. There, the catalyst was activated at 900 °C for 1 h in 100 sccm H_2 flow and CNTs were synthesized for 1 h at the growth temperature of 600 °C for 20Fe : 20Ni : 60Al_2O_3 catalyst and 800 °C for 15Co : 15Mo : 70MgO catalyst, respectively, by flowing 10/100 sccm of C_2H_2/H_2.

The growth of SiC nanorods was also carried out in the same RTCVD reactor, according to the following procedure. Prior to the

growth of SiC nanorods, the Si substrate loaded with 50Fe : 50Co catalysts was placed on the base area of a quartz plate and fixed in the central hot region of the horizontal quartz tube reactor. The metal catalysts were activated at 500 °C for 1 h in H_2 flows (100 sccm). CNTs were grown over the activated catalysts at 600 °C for 5 min with C_2H_2/H_2 (10/100 sccm) and subsequently were reacted with 1.0 sccm tetramethylsilane (TMS) diluted with 200 sccm H_2 for 60 min at 1,100 °C.

The structural and optical properties of the grown micro- and nano-crystals were investigated using scanning electron microscopy (SEM), X-ary diffraction (XRD), transmission electron microscopy (TEM), fourier transform infrared spectroscopy (FT-IR), FT-Raman and photoluminescence (PL) spectroscopy.

RESULS AND DISCUSSION

1. Growth of GaN Micro-Crystals

Fig. 2 shows the growth rate of the GaN crystals as a function of growth temperature in the presence and absence of Ni-mesh catalyst. The growth rate of the GaN crystals increases as the reaction temperature rises from 1,000 to 1,100 °C and the dependency of the growth rate on the temperature is much more significant in the presence of Ni catalyst. For 1,100 °C, the growth rate of GaN micro-crystals grown in the presence of Ni catalyst is over 9 times higher than those grown in the absence of the catalyst. This result demonstrates that Ni-metal acts as an active catalyst in the growth of the GaN crystal. It is thought that the Ni-mesh catalyst enhances the decomposition of NH_3 gas into chemically active nitrogen species and speeds up the reaction of gallium with NH_3 by reducing the activation energy, resulting in the increase of the GaN crystal growth rate.

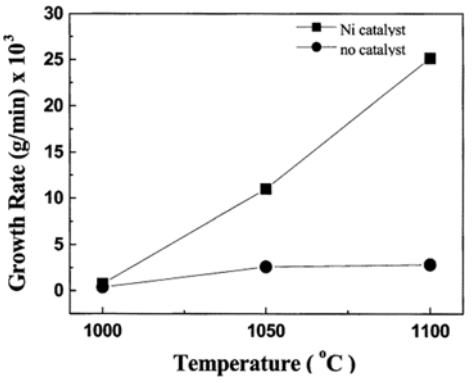

Fig. 2. The growth rate of GaN micro-crystals as a function of growth temperature at 1 atm with 50 sccm NH_3 (■: in the presence and ●: absence of Ni-mesh catalyst).

Crystalline quality of GaN micro-crystals grown using the Ni-mesh catalyst was investigated by TEM. The GaN crystals were grown at 1,000 °C and 1 atm with 50 sccm NH_3. Figs. 3(a) and (b) show the dark-field micrographs and the corresponding selected

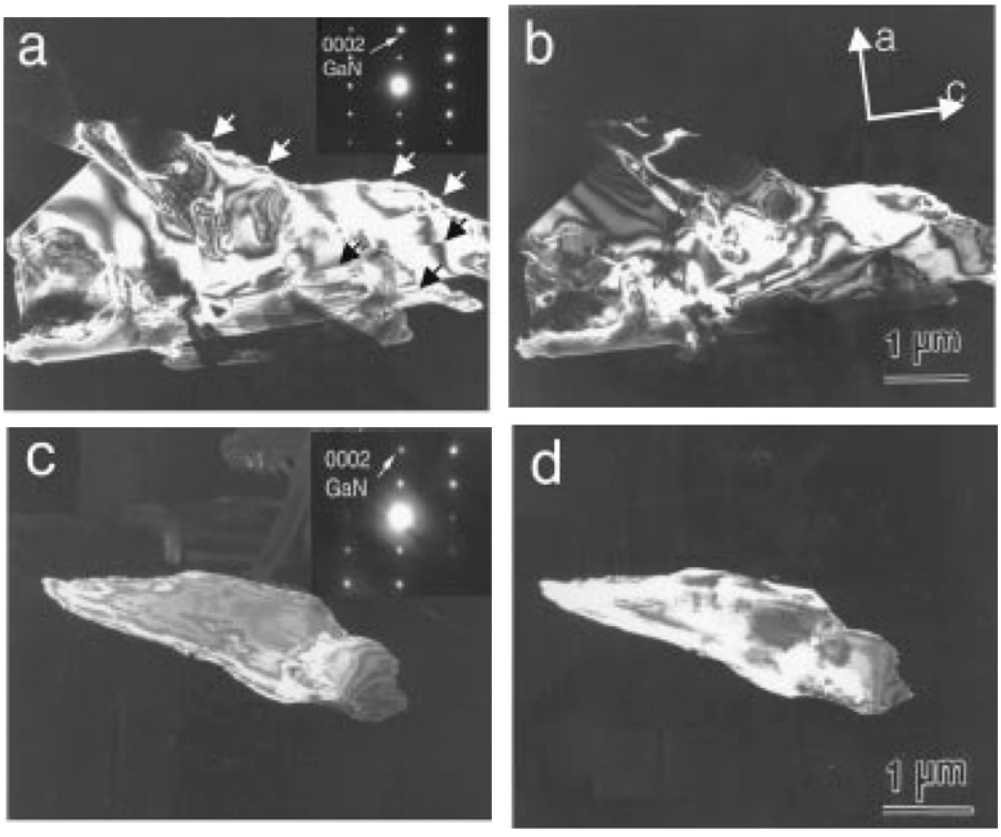

Fig. 3. The dark-field micrographs and the corresponding selected area diffraction pattern (SADP) along the electron beam direction B=[01$\bar{1}$0] with the reflection vectors g=0002 (a, c) and g=[$\bar{2}$110] (b, d) for GaN micro-crystals grown (a, b) with and (c, d) without Ni catalyst, respectively. The GaN crystals were grown at 1,000 °C and 1 atm with 50 sccm NH_3 and the GaN nanowires were grown on Si wafer loaded Ni catalyst at 910 °C and 1 atm for 5 hr with 20 sccm NH_3.

area diffraction pattern (SADP) along the electron beam direction B=[01$\bar{1}$0] with the reflection vectors g=0002 (a) and g=$\bar{2}$110 (b), respectively. It should be noted that the crystal is about 6 μm long and 2 μm wide in size. All the GaN crystals observed in the present study by SADP are identified to have the 2H hexagonal structure with rod crystal, i.e., the crystal's length and width correspond to the c- and a-axis of hexagonal structure, respectively. Dark field micrographs show that the crystal consists of a single crystal without any grain boundary, although some fringes, due to differences of crystal thickness, are observed. Dislocations identified as the major defect in epitaxial GaN films [Cherns et al., 1997] grown on various substrates having the Burgers vectors b=1/3[$\bar{2}$110], b=[0001] and b=1/3[$\bar{2}$113] are not observed from our grown GaN crystals. If such dislocations were found in the present GaN crystal, they should appear with the reflection vector either g=0002 [Fig. 3(a)] or g=$\bar{2}$110 [Fig. 3(b)]. However, this is not the case in the present TEM micrographs. Thus, it can be concluded that most of the GaN crystals exhibit a dislocation free structure, which indicates they experience no strain during the growth process.

For comparison, the dark-field micrographs and the corresponding SADP for GaN micro-crystals grown without the Ni-mesh catalyst were observed as shown in Fig. 3(c) and (d). It should be noted that the crystal size is greatly decreased compared to sample A, i.e., about 3 μm long and 1 μm wide. Dislocations and other defects are not observed when imaged with either g=0002 [Fig. 3(c)] or g=$\bar{2}$110 [Fig. 3(d)] as in the crystal observed in Fig. 3(a) and (b). In Fig. 3(c), lines parallel to the c- and a-axis directions, as well as steps parallel to the basal plane of the hexagonal unit, are clearly observed (as indicated by arrows). It is assumed that they stem from the trace of growth terrace of hexagonal GaN.

PL measurements were performed for the GaN micro-crystals grown using the Ni catalyst. The excitation source was the 325-nm line of He-Cd laser with a 15 mW power focused to an approximately 0.5-mm-diameter spot. The PL from GaN was dispersed and detected by 1 m double-grating monochromator and a photon counting system, respectively. The PL spectrum measured at 5 K shows a strong band edge emission at the energy position of 3.464 eV, but a deep level yellow emission is almost disappeared as shown in Fig. 4(a). The full width at half maximum (FWHM) is as low as 52 meV, the narrowest for all reported GaN micro-crystals in the previous reports [Park et al., 1998; Shmagin et al., 1997]. Although not presented in this paper, time-resolved photoluminescence (PL) experiments showed that the characteristic times of the integrated PL intensity over the whole spectral range of the peak are τ1=22 and τ2=109 ps for the catalytically grown GaN micro-crystals, comparable to the previously reported value for bulk GaN [Hess et al., 1998]. This indicates that transition metal catalysts can be effectively used for the growth of high quality semiconductor crystal growth.

2. Growth of GaN Nanowires

Shown in Fig. 5 is scanning electron microscopy (SEM) image for GaN nanowires grown on Si(100) wafer loaded Ni catalyst. It

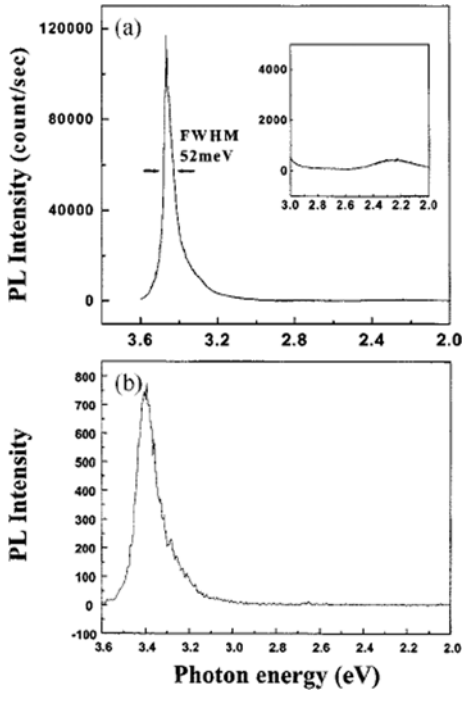

Fig. 4. PL spectrums for (a) GaN micro-crystals and (b) GaN nanowires. The GaN micro-crystals and nanowires were grown at the same condition of Fig. 3.

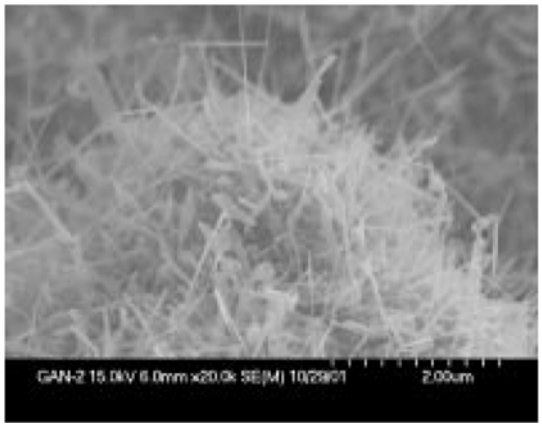

Fig. 5. SEM image for GaN nanowires. The GaN nanowires were grown at the same condition of Fig. 3.

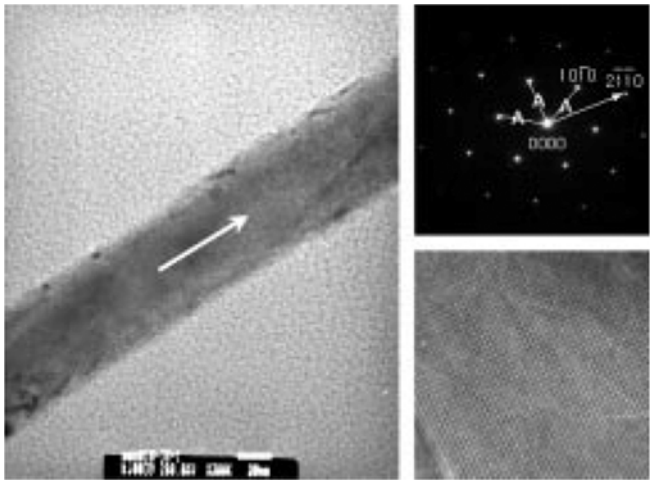

Fig. 6. TEM image and the corresponding SADP for GaN nanowires. The GaN nanowires were grown at the same condition of Fig. 3.

is seen that high density GaN nanowires are grown across the Si substrate. The diameter of the GaN nanowires is in the range of 30-50 nm. The growth of GaN nanowires was also carried out in the absence of Ni catalyst on Si substrate. But no evidence for the growth of the GaN nanowires was found from SEM measurements. Instead of the growth of GaN nanowires, the deposition of hexagonal shaped GaN crystal particles was observed on the Si surface, as reported in the previously reported papers [Park et al., 2000].

Fig. 6 shows the HRTEM image with SADP for the GaN nanowires. The resulting nanowires have diameters in the range of 30-50 nm. No defects between contrast bands are found in the HRTEM image. The clear lattice fringes in this image confirm that a high quality single-crystal structure of the nanowires is grown when Ni metal is applied as catalysts. Also noted in the image is that the $[2\bar{1}\bar{1}0]$ direction was parallel to the long axis of the wires, indicating that $[2\bar{1}\bar{1}0]$ direction is the fast-growth direction for GaN nanowires. The inset of Fig. 6 shows a selected-area electron diffraction pattern of the nanowire that can be indexed to the reflection of hexagonal GaN crystals along [001] directions. TEM measurements show that most of the wires grow along $[2\bar{1}\bar{1}0]$ consistent with earlier experimental results [Duan et al., 2000].

Optical properties of the GaN nanowires were measured using photoluminescence (PL) spectroscopy excited with 325-nm line of He-Cd laser with a 15 mW power focusing to an approximately 0.5 mm-diameter spot. Fig. 4(b) shows a strong band edge emission at the energy position of ~3.4 eV, but a deep level yellow emission is negligible. The full width at half maximum (FWHM) is as low as 53 meV, better than the previously reported value [Chen et al., 2001].

3. Growth of Carbon Nanotubes

Shown in Fig. 7 are the SEM images for CNTs synthesized over 20Fe : 20Ni : $60Al_2O_3$ and 15Co : 15Mo : 70MgO catalysts, respectively. The average diameters of the CNTs grown over 20Fe : 20Ni : $60Al_2O_3$ and 15Co : 15Mo : 70MgO catalysts are about 20 and 10 nm, respectively.

The best way to understand about the quality of CNTs is their Raman spectroscopy measurement. Raman spectroscopy is an effective tool to identify well-graphitized carbon and disordered carbon. In order to clear the fact, we measured the FT-Raman spectra of the carbon products using Nd : YAG laser at a excitation wavelength of 1,064 nm. Fig. 8 shows the FT-Raman spectra for CNTs grown over 20Fe : 20Ni : $60Al_2O_3$ and 15Co : 15Mo : 70MgO catalysts, respectively. Fig. 8(a) clearly show two strong peaks. The peak at around 1,595 cm^{-1} (E_g mode peak) appeared from the formation of well-graphitized CNTs and the other at around 1,285 cm^{-1} (A_g mode peak) arose from the presence of amorphous carbonaceous products with the tubes and disordered carbons [Rao et al., 1997; Choi et al., 2000]. In comparison with the FT-Raman spectra reported for single-wall nanotubes (SWNTs) [Rao et al., 1997] and multi-wall nanotubes (MWNTs) [Choi et al., 2000], the presently observed result for the CNTs grown over 20Fe : 20Ni : $60Al_2O_3$ catalyst coincides with that of MWNTs because the E_g mode peak has no shoulder peaks and no peak for radial breathing mode (RBM) in between

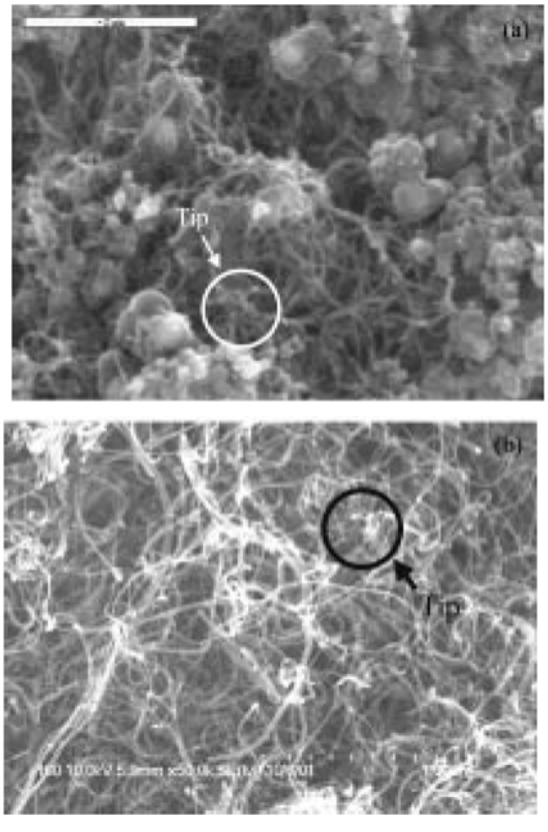

Fig. 7. SEM images for the CNTs grown over (a) 20Fe : 20Ni : $60Al_2O_3$ and (b) 15Co : 15Mo : 70MgO catalysts. The CNTs were synthesized for 1 h at the growth temperature of 600 °C for 20Fe : 20Ni : $60Al_2O_3$ catalyst and 800 °C for 15Co : 15Mo : 70MgO catalyst, respectively, by flowing 10/100 sccm C_2H_2/H_2.

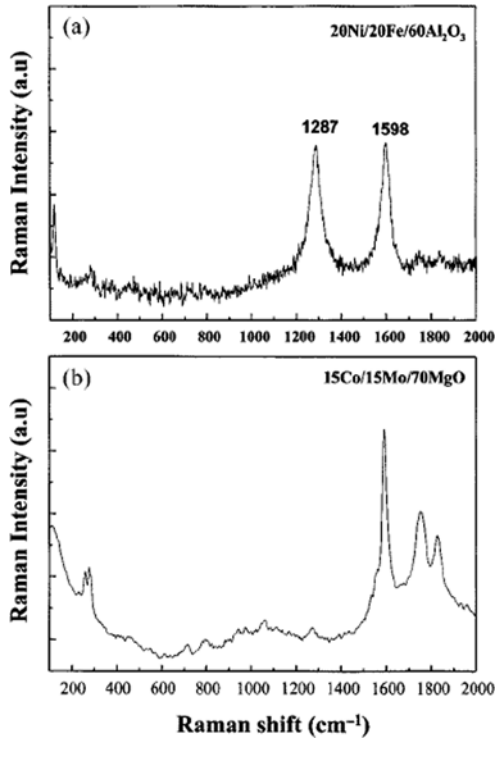

Fig. 8. FT-Raman spectrums of CNTs grown over (a) 20Fe : 20Ni : $60Al_2O_3$ and (b) 15Co : 15Mo : 70MgO catalysts. The CNTs were grown at the same condition of Fig. 7.

150-300 cm^{-1}.

Meanwhile, the CNTs grown over 15Co : 15Mo : 70MgO catalysts shows the characteristic Raman spectrum of SWNTs, shown in Fig. 8(b). The strong Raman band at 1,595 cm^{-1} is observed with three shoulder peaks from the spectrum, as is seen from the typical Raman spectrum of SWNT. The spectrum also shows peaks for radial breathing mode (RBM) in the range of 150-300 cm^{-1}. However, the intensity of peak at 1,285 cm^{-1} arose from MWNTs is almost vanished in this case when comparing with that shown in Fig. 8(a). In the literature on CNTs work, it has generally been reported that MWNTs grow in CVD methods, whereas SWNTs are obtained by arc-discharge and laser ablation methods. But, recently, some research groups including our laboratory have reported the growth of SWNTs by catalytic decomposition of hydrocarbons in CVD reactors. Dai et al. [Dai et al., 1996] have synthesized SWNTs of 1-5 nm diameter by disproportion of CO catalyzed by Mo particles at 1,200 °C. Meanwhile, Peigney et al. [Peigney et al., 1997] have reported the formation of enormous amount of SWNTs and MWNTs of diameter 1.5-15 nm range in CH_4/H_2 media using Fe/Al_2O_3 catalyst. We also proposed the growth of SWNTs over Ni/Al_2O_3 pellet catalyst fabricated by a mechanically mixing method in a RTCVD reactor [Mo et al., 2001]. It is currently well established to grow the SWNTs using CVD techniques [Alvarez et al., 2001].

4. Growth of SiC Nanowires

Fig. 9 shows SEM image for SiC nanorods produced from the CNTs grown for 5 min. As shown in the SEM image, a large quantity of straight or curved nanorods grows across the substrate surface. The average length and diameter of the nanorods are in the ranges of 1-2 μm and 110-130 nm, respectively. The metal catalyst tip was observed at the top of CNTs in the inset of Fig. 9, as can be seen in the previous work [Kibria et al., 2001]. It seems that the metal catalyst tip still remain on the top of the nanorods without a remarkable change after the SiC nanorod growth. This means that the growth of the SiC nanorods is due to the conversion of the CNTs, but not due to a elongated growth on the metal catalyst tips.

Figs. 10(a) and (b) show FT-IR absorption spectra for CNTs and SiC nanorods. The Si-Si and Si-O vibration modes, which are observed at 610 and 1,096 cm^{-1}, originate from the Si substrate [Seo et al., 1994]. A strong absorption band at 796 cm^{-1} of Fig. 10(b) is due to the C-Si stretching vibration mode in the SiC crystalline phase [Yu et al., 2000]. This also indicates that the SiC nanorods are mainly produced by the reaction of the CNTs with TMS. Zigzag weak absorption bands between 1,450 to 1,650 cm^{-1} correspond to the vibration of the carbon framework [Tarasov et al., 2001]. A very weak absorption band at 1,645 cm^{-1} presents the existence of excessive carbons in the CNTs having a crystalline graphite structure [Sun et al., 1999; Lee et al., 2002]. The intensity of the absorption band at 1,096 cm^{-1} decreases for the SiC nanorod sample because the Si-O bond in the CNT grown on Si substrate might be consumed by the reduction with H_2 at higher temperature during the reaction. The IR observation manifests that the formation of the SiC nanorods are produced by the conversion of the CNTs.

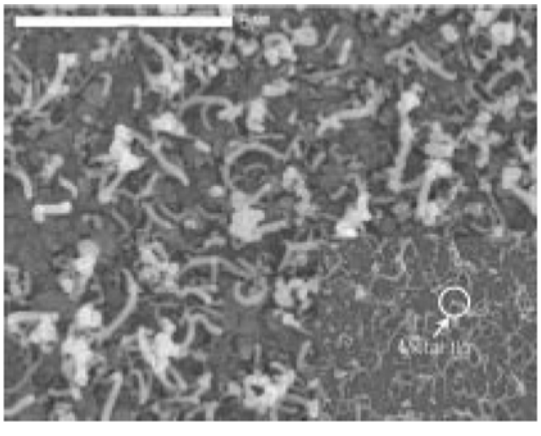

Fig. 9. SEM images of SiC nanorods with the corresponding CNTs. The SiC nanorods were grown on Fe/Co catalyst loaded Si wafer by the reaction of CNTs grown for 5 min at 600 °C with TMS/ H_2 (1.0/200 sccm) for 60 min at 1,100 °C.

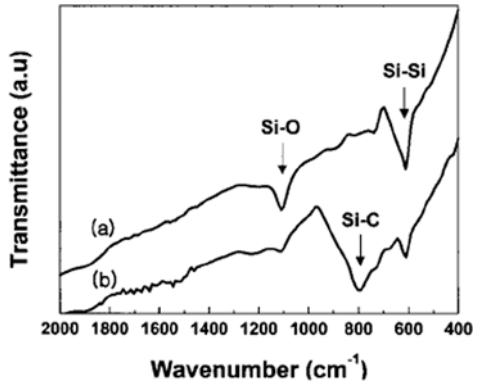

Fig. 10. FT-IR spectrums for CNTs (a) and SiC nanorods (b). The SiC nanorods were grown at the same condition of Fig. 9.

Fig. 11 shows the FT-Raman spectrum for SiC nanorods. The CNT related peaks are still observed at 1,295, 1,606 and 2,565 cm^{-1} although their peak intensities are significantly reduced in the figure, which is attributed to the remnant CNTs unreacted completely [Zhang et al., 1999]. Besides, the peak intensity at 527 cm^{-1} becomes more apparent in the figure. It is thought that these results are caused by the continuous conversion of the CNTs into SiC nanorods and hydrogen etching of carbonaceous species from the Si substrate during the reaction. A sharp peak at 940 cm^{-1} is the longitudinal optical (LO) mode of the SiC lattice and the peak at 808 cm^{-1} is as the transverse optical (TO) mode. The Raman spectroscopic data indicate

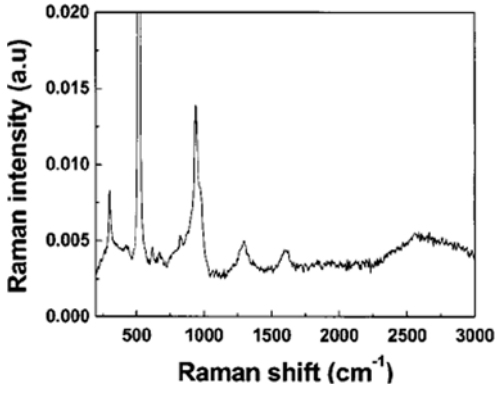

Fig. 11. Raman spectrum for SiC nanorods. The SiC nanorods were grown at the same condition of Fig. 9.

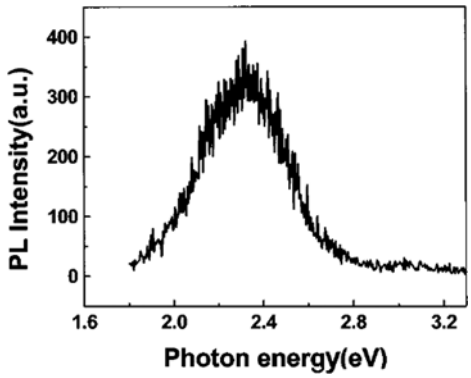

Fig. 12. Photoluminescence spectrum of SiC nanorods measured at 10 K. The SiC nanorods were grown at the same condition of Fig. 9.

again the growth of SiC by the reaction of the CNTs with TMS. Furthermore, a peak at 880 cm^{-1} observed between these two main peaks is due to the formation of SiC nanorods reported in the previous work [Zhang et al., 1999]. The Raman spectrum is different from that of the bulk SiC or thick SiC film. The bulk β-SiC is a zinc-blende structure which has a TO mode at 796 cm^{-1} and LO mode at 972 cm^{-1}, respectively [Zhang et al., 1999]. It is speculated that the frequency shift of our sample is due to the effect of quantum confinement or the effect of defects on the Raman scattering of optical phonons.

Shown in Fig. 12 is a typical PL spectrum for the SiC nanorods. The PL spectrum was measured at 10 K by using 325 nm line from a He-Cd laser with 50 mW output power and corrected for the spectral response of the instrument. The PL has a peak at 2.32 eV and a full width at the half-maximum (FWHM) is approximately 0.45 eV. It is noted that the PL peak energy is a little higher than the room temperature optical bandgap energy of β-SiC (2.2 eV) [Yu et al., 2000]. It is considered that the shift of the PL peak emission energy toward blue is due to the quantum size effect of the nanocrystallites. The large FWHM value of the PL peak might be attributed to a spread in the size of the nanocrystallites. Chen et al. [Chen et al., 2000] attributed the origin of the observed PL peaks in the range from 1.9 to 2.3 eV to states associated with structural defects in crystalline SiC or SiC-Si interface. They assumed these defects consist of distorted and weakly bonded atoms such as Si-Si, C-C and Si-C with longer bonding lengths or disturbed bonding angles. The bonding energy of these atoms was generally lower than that of the normally bonded atoms and the bonds can be broken by the absorption of a higher energy.

CONCLUSIONS

GaN micro- and nano-crystal structures, carbon nanaotubes, and SiC nanostructures were grown using transition metal catalysts to introduce the catalytic growth of semiconductor crystals. GaN microcrystals were catalytically grown using Ni-mesh by direct reaction of gallium and ammonia. At 1,100 °C, the growth rate of the GaN crystals in the presence of Ni catalyst was almost nine times higher than that in the absence of the catalyst. The structural characterization of the GaN crystal showed the growth of dislocation free hexagonal GaN single crystal. The GaN nanowires were grown over Si(100) wafer loaded with Ni catalyst. The grown GaN nanowires range from 30 to 50 nm in diameter and were identified to have the 6H hexagonal structure with the growth along [2110] direction. CNTs were synthesized over 20Fe : 20Ni : 60Al_2O_3 and 15Co : 15Mo : 70MgO bimetal supported catalysts. It was found that MWNTs were grown over 20Fe : 20Ni : 60Al_2O_3 catalyst, whereas SWNT were grown over 15Co : 15Mo : 70MgO catalyst. The average diameter of the CNTs ranged from 10-20 nm. This indicated that the selection of catalysts was essential to control the CNT structure on purpose. Silicon carbide (SiC) nanorods were grown over on Si wafer loaded with Fe/Co metal catalyst through a two-step reaction scheme. The SiC nanorods grown were identified to be β-SiC. The distribution of length and diameter of the SiC nanorods were consistent with the starting CNTs.

ACKNOWLEDGEMENT

This work was supported by grant No.(1999-2-114-008-5) from the interdisciplinary research program of the KOSEF.

REFERENCES

Akasaki, I. and Amano, H., "Crystal Growth and Conductivity Control of Group III Nitride Semiconductors and Their Application to Short Wavelength Light Emitters," *Jpn. J. Appl. Phys.*, **36**, 5393 (1997).

Alvarez, W. E., Kitiyanan, B., Borgna, A. and Resasco, D. E., "Synergism of Co and Mo in the Catalytic Production of Single-wall Carbon Nanotubes by Decomposition of CO," *Carbon*, **39**, 547 (2001).

Bethune, D. S., Kiang, C. H., De Vries, M. S., Gorman, G., Savoy, R., Vazquez, J. and Beyers, R., "Cobalt-Catalysed Growth of Carbon Nanotubes with Single-Atomic-Layer Walls," *Nature*, **363**, 605 (1993).

Chen, C.-C., Yeh, C.-C., Chen, C.-H., Yu, M.-Y., Liu, H.-L., Wu, J.-J., Chen, K.-H., Chen, L.-C., Peng, J.-Y. and Chen, Y.-F., "Catalytic Growth and Characterization of Gallium Nitride Nanowires," *J. Am. Chem. Soc.*, **123**, 2791 (2001).

Chen, Z. M., Ma, J. P., Yu, M. B., Wang, J. N., Ge, W. K. and Woo, P. W., "Light Induced Luminescence Centers in Porous SiC Prepared from Nano-Crystalline SiC Grown on Si by Hot Filament Chemical Vapor Deposition," *Materials Science and Engineering B*, **75**, 180 (2000).

Cherns, D., Young, W. T., Steeds, J. W., Ponce, F. A. and Nakamura, S., "Observation of Coreless Dislocations in α-GaN," *J. Crystal Growth*, **178**, 201 (1997).

Choi, Y. C., Bae, D. J., Lee, Y. H., Lee, B. S., Han, I. T., Choi, W. B., Lee, N. S. and Kim, J. M., "Low Temperature Synthesis of Carbon Nanotubes by Microwave Plasma-enhanced Chemical Vapor Deposition," *Synth. Met.*, **108**, 159 (2000).

Dai, H., Rinzler, A. G., Nikolaev, P., Thess, A., Colbert, D. T. and Smalley, R. E., "Single-wall Nanotubes Produced by Metal-catalyzed Disproportionation of Carbon Monoxide," *Chem. Phys. Lett.*, **260**, 471 (1996).

Derycke, V., Martel, R., Appenzeller, J. and Avouris, Ph., "Carbon Nanotube Inter- and Intramolecular Logic Gates," *Nano Letters*, **1**, 453 (2001).

Dillon, A. C., Jones, K. M., Bekkedahl, T. A., Kiang, C. H., Bethune, D. S. and Heben, M. J., "Storage of Hydrogen in Single-walled Car-

bon Nanotubes," *Nature*, **386**, 377 (1997).
Duan, X. F. and Lieber, C. M., "Laser-Assisted Catalytic Growth of Single Crystal GaN Nanowires," *J. Am. Chem. Soc.*, **122**, 188 (2000).
Gonsalves, K. E., Rangarajan, S. D., Carlson, G., Kumar, J., Yang, K., Benaissa, M. and José-Yacanán, M., "Optical and Microstructural Characterization of Chemically Synthesized Gallium Nitride Nanopowders," *Appl. Phys. Lett.*, **71**, 2175 (1997).
Gu, S., Ahang, L., Zhang, R., Wicks, G. W. and Kuech, T. F., "Epitaxial Lateral Overgrowth of GaN on Si Substrates by Hydride Vapor Phase Epitaxy," Proc. Int. Workshop on Nitride Semiconductors, 23-26 (2000).
Guo, T., Nikolaev, P., Thess, A., Colbert, D. T. and Smalley, R. E., "Catalytic Growth of Single-Walled Nanotubes by Laser Vaporization," *Chem. Phys. Lett.*, **243**, 49 (1995).
Hassanien, A., Tokumoto, M., Kumazawa, Y., Kataura, H., Maniwa, Y., Suzuki, S. and Achiba, Y., "Atomic Structure and Electronic Properties of Single-wall Carbon Nanotubes Probed by Scanning Tunneling Microscope at Room Temperature," *Appl. Phys. Lett.*, **73**, 3839 (1998).
He, M., Zhou, P., Mohammad, S. N., Harris, G. L., Halpern, J. B., Jacobs, R., Sarney, W. L. and Salamanca-Riba, L., "Growth of GaN Nanowires by Direct Reaction of Ga with NH_3," *J. Crystal Growth*, **231**, 357 (2001).
Hess, S., Walraet, F., Taylor, R. A., Ryan, J. F., Beaumont, B. and Gibart, P., "Dynamics of Resonantly Excited Excitons in GaN," *Phys. Rev. B*, **58**, R15973 (1998).
Iijima, S., "Helical Microtubules of Graphitic Carbon," *Nature*, **354**, 56 (1991).
Im, J. S. and Sposili, R. S., "Crystalline Si Films for Integrated Active-Matrix Liquid-Crystal Displays," *MRS Bulletin*, **March**, 39 (1996).
Iijima, S. and Ichihashi, T., "Single-Shell Carbon Nanotubes of 1-nm Diameter," *Nature*, **363**, 603 (1993).
Ivanov, V., Fonseca, A., Nagy, J. B., Lucas, A., Lambin, P., Bernaerts, D. and Zhang, X. B., "Catalytic Production and Purification of Nanotubules Having Fullerene-Scale Diameters," *Carbon*, **33**, 1727 (1995).
Iverson, R. B. and Reif, R., "Recrystallization of Amorphized Polycrystalline Silicon Films on SiO_2: Temperature Dependence of the Crystallization Parameters," *J. Appl. Phys.*, **62**, 1675 (1987).
Jang, J., Oh, J. Y., Kim, S. K., Choi, Y. J., Yoon, S. Y. and Kim, C. O., "Electric-Field-Enhanced Crystallization of Amorphous Silicon," *Nature*, **395**, 481 (1998).
Kibria, A. K. M., Fazle, Mo, Y. H., Park, K. S. and Nahm, K. S., "Electrochemical Hydrogen Storage Behaviors of CVD, AD and LA Grown Carbon Nanotubes in KOH Medium," *Int. J. Hydrogen. Energy*, **26**, 823 (2001).
Kibria, A. K. M., Fazle, Mo, Y. H. and Nahm, K. S., "Synthesis of Carbon Nanotubes over Nickel-iron Catalysts Supported on Alumina Under Controlled Condition," *Catalysis Letters*, **71**, 229 (2001).
Kibria, A. K. M., Fazle, Mo, Y. H., Yun, M. H., Kim, M. J. and Nahm, K. S., "Effects of Bimetallic Supported Catalysts and Growth Parameters on the Growth Density and Diameter of Carbon Nanotubes," *Korean J. Chem. Eng.*, **18**, 208 (2001).
Kim, W., Aktas, O., Salvador, A., Botchkarev, A., Sverdlov, B., Mohammad, S. N. and Morkoç, H., "MBE Grown High Quality GaN Films and Devices," *Solid-State Electronics*, **41**, 169 (1997).
Koo, C. M., Kim, M. J., Choi, M. H., Kim, S. O. and Chung, I. J., "The Effect of Molecular Weight of pp-g-MA/Layered Silicate the Nanocomposities," *Korean J. Chem. Eng.*, **39**, 635 (2001).
Lee, S. H., Nahm, K. S., Suh, E.-K. and Hong, M. H., "Characterization of Mg-doped GaN Micro-crystals Grown by Direct Reaction of Gallium and Ammonia," *Phys. Stat. Sol.(b)*, **228**, 371 (2001).
Lee, S. J., Kim, M. H., Kim, Y. T. and Chung, G. Y., "Studies on the Preparation of C/SiC Composite as a Catalytic Support by CVI in a Fluidized Bed Reactor," *Korean J. Chem. Eng.*, **19**, 167 (2002).
Maser, W. K., Bernier, P., Lambert, J. M., Stephan, O., Ajayan, P. M., Colliex, C., Brotons, V., Planeix, J. M., Coq, B., Molinie, P. and Lefrant, S., "Elaboration and Characterization of Various Carbon Nanostructures," *Synth. Met.*, **81**, 243 (1996).
Mo, Y. H., Kibria, A. K. M. F. and Nahm, K. S., "The Growth Mechanism of Carbon Nanotubes from Thermal Cracking of Acetylene over Nickel Catalyst Supported on Alumina," *Synth. Met.*, **122**, 443 (2001).
Nahm, K. S., Ahn, S. H. and Lee, S. H., "The Catalystic Growth of GaN Powders," Proc. Int. Workshop on Nitride Semiconductors, 31 (2000).
Park, C. I., Kang, J. H., Kim, K. C., Suh, E.-K., Lim, K. Y. and Nahm, K. S., "Effect of a Buffer Layer on GaN Growth on a Si(111) Substrate with a 3C-SiC Intermediate Layer," *J. Kor. Phys. Soc.*, **37**, 1007 (2000).
Park, Y. J., Son, M. H., Kim, E. K. and Min, S. K., "Formation of GaN Micro-Crystals by the Direct Reaction of NH_3 with a Ga-Melt," *J. Kor. Phys. Soc.*, **32**, 621 (1998).
Peigney, A., Laurent, C., Dobigeon, F. and Rousset, A., "Carbon Nanotubes Grown in-situ by a Novel Catalytic Method," *J. Mater. Res.*, **12**, 613 (1997).
Porowski, S., "High Pressure Growth of GaN - New Prospects for Blue Lasers," *J. Crystal Growth*, **166**, 583 (1996).
Rao, A. M., Richter, E., Bandow, E. S., Chasc, B., Eklund, P. C., Williams, K. A., Fang, S., Subbaswamy, K. R., Menon, M., Thess, A., Smalley, R. E., Dresselhaus, G. and Dresselhaus, M. S., "Diameter-Selective Raman Scattering from Vibrational Modes in Carbon Nanotubes," *Science*, **275**, 187 (1997).
Saito, Y., Yoshikawa, T., Okuda, M., Fujimoto, N., Sumiyama, K., Suzuki, K., Kasuya, A. and Nishina, Y., "Carbon Nanocapsules Encaging Metals and Carbides," *J. Phys. Chem. Solids*, **54**, 1849 (1993).
Seo, Y. H., Nahm, K. S., An, M. H., Suh, E.-K., Lee, Y. H., Lee, K. B. and Lee, H. J., "Formation Mechanism and Pore Size Control of Light-Emitting Porous Silicon," *Jpn. J. Appl. Phys. Part 1*, **33**, 6425 (1994).
Seo, Y. H., Nahm, K. S., Suh, E.-K., Lee, H. J. and Hwang, Y. G., "Growth Mechanism of 3C-SiC(111) Films on Si Using Tetramethylsilane by Rapid Thermal Chemical Vapor Deposition," *J. Vac. Sci. & Techn. A.*, **15**, 2226 (1997).
Shibata, M., Furuya, T., Sakaguchi, H. and Kuma, S., "Synthesis of Gallium Nitride by Ammonia Injection into Gallium Melt," *J. Crystal Growth*, **196**, 47 (1999).
Shmagin, I. K., Muth, J. F., Lee, J. H., Kolbas, R. M., Balkas, C. M., Sitar, Z. and Davis, R. F., "Optical Metastability in Bulk GaN Single Crystals," *Appl. Phys. Lett.*, **71**, 455 (1997).
Sun, Y., Miyasato, T. and Wigmore, J. K., "Characterization of Excess Carbon in Cubic SiC Films by Infrared Absorption," *J. Appl. Phys.*, **85**, 3377 (1999).
Tarasov, B. P., Shulga, Yu. M., Fokin, V. N., Vasilets, V. N., Shulga, N. Yu., Schur, D. V. and Yartys, V. A., "Deuterofullerene $C_{60}D_{24}$ Studied

by XRD, IR and XPS," *J. Alloys and Compounds*, **314**, 296 (2001).
Xie, Y., Qian, Y., Wang, W., Zhang, S. and Zhang, Y., "A Benzene-Thermal Synthetic Route to Nanocrystalline GaN," *Science*, **272**, 1926 (1996).
Yoon, S. Y., Park, S. J., Kim, K. H. and Jang, J., "Metal-Induced Crystallization of Amorphous Silicon," *Thin Solid Films*, **383**, 34 (2001).
Yu, M. B., Rusil, Yoon, S. F., Xu, S. J., Chew, K., Cui, J., Ahn, J. and Zhang, Q., "Hydrogenated Nanocrystalline Silicon Carbide Films Synthesized by ECR-CVD and Its Intense Visible Photoluminescence at Room Temperature," *Thin Solid Films*, **377**, 177 (2000).
Zhang, S.-L., Zhu, B.-F., Huang, F., Yan, Y., Shang, Er-yi, Fan, S. and Han, W., "Effect of Defects on Optical Phonon Raman Spectra in SiC Nanorods," *Solid State Communications*, **111**, 647 (1999).